Location-Aided mMIMO Channel Tracking and Hybrid Beamforming for High-Speed Railway Communications: An Angle-Domain Approach

Kui Xu, *Member, IEEE*, Zhexian Shen, Yurong Wang, and Xiaochen Xia

***Abstract*—Wireless communication for high-speed railways (HSRs) has received considerable attention in recent years. The fast time-varying and doubly selective fading properties of channels pose a substantial threat to the link performance. Meanwhile, the nonnegligible Doppler frequency offset (DFO) resulting from the high-speed motion induces intercarrier interference. In this paper, we propose an angle-domain channel tracking and hybrid beamforming scheme for HSR by investigating the time and spatial properties of channels. A large-scale uniform linear antenna array is applied at the base station to provide high spatial resolution. The DFO is compensated through beam alignment and capturing the precise angular information from signals. Then, the spatial beam gain is tracked during the angle-of-arrival time, which can be used to reconstruct the full-dimensional channel state information. Finally, the hybrid beamforming is used to realize data transmission. The key idea of tracking is, applying a linear Kalman filter to modify the time-varying beam gain, while the main idea of hybrid beamforming is utilizing nonorthogonal beams to compress the channel dimension and decrease the computational complexity. The superiority of the proposed scheme is evaluated through simulations.**

***Index Terms*—Angle-domain (AD) channel tracking, Doppler frequency offset (DFO), high-speed railways (HSR) communication, hybrid beamforming, massive multi-input multi-output (mMIMO).**

I. Introduction

With the increasing demand for high-quality railway service, high-speed railways (HSRs) are rapidly developing around the world. In China, the total kilometers of operating HSRs has increased to 25 000 km in 2018. Due to the rapid development of HSRs, wireless communication for HSR applications is receiving widespread attention [1]–[3]. The challenges and opportunities with high-mobility communications was discussed in [1]. The evolution from global system for mobile communications to long-term evolution railway for HSR wireless communications was suggested in [2]. Moreover, as one of the key technologies in fifth-generation (5G) communications, massive multi-input multi-output (mMIMO) technology explores the diversity and multiplexing gain, and enhances the spectral efficiency (SE) of wireless networks [4]–[7]. The application of mMIMO is considered to potentially bring a significant performance gain to HSR communications [8]–[11].

In contrast to urban cellular systems, many challenging problems exist in HSR scenarios. The electromagnetic shielding from the carriage results in a strong penetration loss of signals, and it is difficult to build a direct link between the base station (BS) and users [12], [13]. The overhead line poles along the rail periodically block the line-of-sight (LoS) path and act as a static and periodic scatters [14]. The high mobility of trains not only results in a sharp decrease in coherence time (CT) but also leads to a nonnegligible Doppler shift, which causes intercarrier interference (ICI) and serious performance loss [15]–[18]. In addition, the fast time-varying and doubly selective fading properties of channels make it difficult to acquire channel state information (CSI) at a low cost [10], [19]. Designing the training and transmission schemes appears to be difficult. Fortunately, some special characteristics appear in the HSR scenario that help simplify the system design. In viaduct and cutting scenarios, the LoS path dominates the HSR channel, while the channel gain of non-LoS (NLoS) paths is considerably weaker [20]. According to the measurement of angular characteristics, the angular spread (AS) in viaduct and cutting environments is smaller than that in urban environments [21], [22].

In recent years, many works have been conducted toward the development of HSR communications. In [10], a position-aided channel estimation scheme was proposed, whereby only a portion of the transmit antennas send pilot signals, while the full-dimensional (FD) channel can be estimated by using pilot signals together with antenna position information based on spatial–temporal coherence. In [23], a sparse channel estimation approach for MIMO systems in high-mobility scenarios was investigated, which greatly avoids estimating a large quantity of channel coefficients by utilizing sparsity in the time-angle domain. Based on temporal coherence, a Kalman filter (KF) was applied to improve the accuracy of channel estimation [24], [25]. An extended KF scheme was proposed to track the channel with less training overhead by exploiting the temporal coherence [12]. Except temporal coherence, spatial coherence was also utilized to design channel tracking schemes [26]–[28]. In [26], [27], an unscented KF (UKF) scheme was applied to track the position of high-mobility targets and thus reduce training overhead. Paper [28] studied the position tracking of high-speed trains in 5G new radio (NR) by using synchronization signals. To realize the position tracking, directional antennas were fixed on remote radio heads (RRHs) and the train. In addition, the beamforming methods for the HSR scenario were well designed [8], [9], [29]. An effective downlink multiuser beamforming was designed [29].

Manuscript received August 14, 2018; revised January 3, 2019 and February 19, 2019; accepted April 11, 2019. This work was supported in part by the National Natural Science Foundation of China under Grant 61671472 and Grant 61771486 and in part by the Jiangsu Province Natural Science Foundation under Grant BK20160079. *(Corresponding author: Zhexian Shen.)*

The authors are with the Institute of Communications Engineering, Army Engineering University of PLA, Nanjing 210007, China.

Digital Object Identifier 10.1109/JSYST.2019.2911296

Paper [8] considered simplifying the complexity of beamforming in the mMIMO HSR system and presented a location-aided fast beamforming scheme that is robust to location errors. In [9], a practical umbrella-shaped beamforming scheme with the transmit diversity of mMIMO was proposed to significantly reduce the system complexity and reinforce the signal strength in the boundary region between two cells.

When considering the application of mMIMO to HSR communication systems, the main problem is that the pilot overhead and training complexity of high-dimensional channels are not taken into account. To retain the orthogonality of users, the length of the pilot sequence for a time-division duplex (TDD) mMIMO system should be larger than the number of users [31], whereas for a frequency-division duplex system, the length will be even larger than the number of antennas, which is unacceptable [32]. In addition, the increasing training time occupies much of the resources and increases the burden of the BS. Although the spatial basis expansion model can be applied to transform channels into the beam domain (BD) to decrease the dimension [33], [34], in shortened CT, there is not enough time to acquire the channel coherence matrix. Meanwhile, the beamforming complexity should be taken into account, which is nonnegligible, particularly in HSR scenarios.

In this paper, we focus on the design of an HSR communication scheme with a large-scale uniform linear antenna array (ULA). We consider a practical wireless propagation environment and take pilot overhead and hardware complexity into account. A novel Doppler frequency offset (DFO) compensation method is designed, which utilizes the high spatial resolution of the array and beam alignment. Based on spatial angular information, an angle-domain (AD) tracking scheme is proposed to track the beam gain and recover the CSI. Finally, a hybrid beamforming is introduced to decrease the hardware overhead and computational complexity. Compared with tracking nonlinearly varying angle of arrival (AOA) [26], [27], the proposed AD scheme aims at tracking linearly varying beam gain by using temporal coherence of channel. Thus the computational complexity is reduced. In addition, the angular information is estimated from normal pilot signals, which will be further used for tracking channels, no additional signals are needed, e.g., synchronization signals [28], [29]. The contributions of this work are summarized as follows.

1) An AD beam alignment method is applied to acquire a precise AOA, which can be obtained by applying a fast Fourier transform (FFT) and phase rotation. By utilizing beam alignment, DFO can be directly compensated.
2) Based on temporal coherence, a KF-based multipath channel tracking scheme is proposed, which is self-adaptive to CSI variance. The tracking scheme is further expanded to the AD to significantly decrease the pilot overhead and computational complexity.
3) In the data transmission phase, a hybrid beamforming scheme is proposed to compress the channel dimension and keep low complexity, which is composed of DFO compensation, angular beamforming, and BD precoding. Compared with the linear method, the hybrid beamforming scheme requires considerably less computations while retaining high throughput.

The remainder of this paper is organized as follows. Section II introduces the channel characteristics. Section III presents the joint beam alignment and DFO compensation method. In Section IV, we present the multipath channel tracking scheme and AD tracking scheme. In Section V, we introduce data transmission during uplink and downlink. Section VI compares the pilot overhead and computational complexity among different CSI acquisition and beamforming methods. Section VII presents the numerical simulation results. Finally, the conclusion is presented in Section VIII.

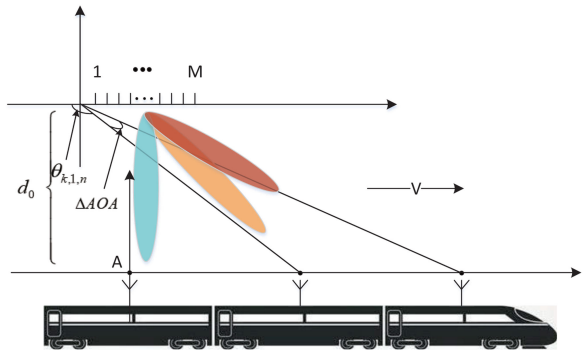

Fig. 1. System model of HSR communications with mMIMO.

II. System Model and Channel Characteristics

Consider an HSR scenario in which the BS is equipped with a ULA with M elements. Due to the electromagnetic shielding provided by the carriages, two-hop links are established between the BS and users through $K(K \ll M)$ independent terminal equipments (TEs) [13].[1] To simplify the model, the cofrequency interference from other cells or RRHs is not considered.[2] Signal propagation between the BS and TEs is mainly considered, and an illustration of the system model is presented in Fig. 1.

Recent studies have shown that in an HSR wireless propagation environment, LoS paths are much stronger than NLoS paths, especially in the viaduct scenario [20]–[22]. According to the measurement in viaduct environment, the strength of K-factor can reach as high as 20 dB when the relative horizontal distance between transmitter and receiver reaches 500 m [30]. Although channels in U-shape cutting scenario have lower K-factor, wireless channels are still dominated by LoS paths.[3] In this paper, we mainly focus on the wireless channels in the above two scenarios. According to the multipath fading model [16], [35]–[37], the time-varying channel from the kth TE to the BS in the nth CT is modeled as

$$\begin{aligned}\mathbf{h}_{k,n,f_D} &= e^{j\phi_n}\sum_{l=1}^{L} e^{j\phi_{f_{D,l,n}}}\cdot\psi_l\alpha_{k,l,n}\mathbf{a}\left(\theta_{k,l,n}\right)\odot\mathbf{b}_{k,l,n}\\ &= \sum_{l=1}^{L} e^{j\left(\phi_n+\phi_{f_{D,l,n}}\right)}\cdot\psi_l\alpha_{k,l,n}\mathbf{O}\left(f_{D,l,n}\right)\mathbf{a}\left(\theta_{k,l,n}\right)\end{aligned} \tag{1}$$

where ϕ_n denotes the phase caused by the carrier frequency, $\phi_{f_D,l,n}$ denotes the absolute phase offset resulting from Doppler

[1] At the BS side, both analog and digital beamforming are available [35]. However, based on the limited resources and processing capacity, more simple antennas are equipped at the train side [28]. Here, each TE can be considered a single omnidirectional antenna.

[2] The extra gain from the antenna array provides greater coverage and stronger signals without the help of RRH. Meanwhile, the spatial resolution is significantly enhanced. In this condition, the spatial orthogonality of beams is guaranteed, and interference from other transmission points is canceled.

[3] Under deep U-shape cutting scenario, there does not exist strong LoS path.

TABLE I
SOME IMPORTANT VARIABLES FOR PROBLEM DESCRIPTION IN THIS PAPER

Variable	Description
$\phi_{f_{D,l,n}}$, $\mathbf{O}\left(f_{D,l,n}\right)$	the absolute DFO and relative DFO, respectively
$f_{D,l,n}$	the Doppler shift of the lth path
$\theta_{k,l,n}$, $\theta_{k,n}$, $\theta'_{k,n}$	AOA for the lth path, azimuth angle of TE and actual AOA of signal, respectively
M, K	the number of ULA elements and TEs, respectively
N, N_m	the oversampling times and tracking period, respectively
ρ_l	the temporal correlation coefficient
$\{B^{r_0}\}$	the beam set containing K aligned beams
$\tilde{\mathbf{h}}_{k,n}^{r_0}$, $\left(\tilde{\mathbf{h}}_{k,n}^{r_0}\right)_{i_k}$, $\tilde{\mathbf{H}}_n^{\{B_{r_0}\}}$	modified DFT of channel, beam gain value of channel and beam domain channel, respectively

shift for the lth path, and $\phi_{f_{D,l,n}} = 2\pi f_{D,l,n} nT$. T is the length for one CT. The Doppler shift for the lth path is defined as $f_{D,l,n} = \frac{v}{\lambda}\cos(\theta_{k,l,n})$, where v and λ are the velocity of the train and the wavelength of the carrier frequency, respectively. $\theta_{k,l,n}$ is the AOA for the lth path. Assume that the first path ($l = 1$) denotes the LoS component, while the other paths ($l \geq 2$) denote the NLoS components. Since high Rician factor exists in the scenario, the weight coefficient ψ_l is defined as

$$\psi_l = \begin{cases} \sqrt{\frac{\mathcal{K}}{\mathcal{K}+1}}, & l = 1 \\ \sqrt{\frac{1}{(\mathcal{K}+1)(L-1)}}, & l \geq 2 \end{cases} \tag{2}$$

where $\mathcal{K}$ is the Rician factor. $\alpha_{k,l,n}$ is the complex gain, which complies with a zero-mean complex Gaussian distribution with variance $\sigma^2_{k,l,n}$. $\mathbf{a}(\theta_{k,l,n})$ is the steering vector, which is defined as $\mathbf{a}(\theta_{k,l,n}) = [1, e^{j2\pi\frac{d}{\lambda}\cos(\theta_{k,l,n})}, \ldots, e^{j2\pi(M-1)\frac{d}{\lambda}\cos(\theta_{k,l,n})}]$, d is the antenna spacing. $\mathbf{b}_{k,l,n}$ denotes the relative Doppler phase offset vector, which is expressed as $\mathbf{b}_{k,l,n} = [1, e^{j2\pi f_{D,l}t}, \ldots, e^{j2\pi(M-1)f_{D,l}t}]^T$, $\mathbf{O}(f_{D,l,n})$ is defined as $\mathbf{O}(f_{D,l,n}) = diag(1, e^{j2\pi f_{D,l,n}t}, \ldots, e^{j2\pi(M-1)f_{D,l,n}t})$. Note that t is the duration difference resulting from different propagation distances when signals are transmitted to adjacent antenna elements, which can be expressed as $t = \frac{d\cos(\theta_{k,l,n})}{c}$, and "$\odot$" is the Hadamard product. Then the time-varying multipath fading channel model is rewritten as

$$\begin{aligned} \mathbf{h}_{k,n,f_D} &= \sum_{l=1}^{L} e^{j\left(\phi_n + \phi_{f_{D,l,n}}\right)} \\ &\quad \psi_l \alpha_{k,l,n}\left(1, e^{j2\pi s_{l,n}}, \ldots, e^{j2\pi(M-1)s_{l,n}}\right)^T \\ &= \sum_{l=1}^{L} e^{j\left(\phi_n + \phi_{f_{D,l,n}}\right)} \cdot \psi_l \alpha_{k,l,n} \mathbf{a}'\left(s_{l,n}\right) \end{aligned} \tag{3}$$

where $s_{l,n}$ is given by

$$s_{l,n} = \frac{d}{\lambda}\left(1 + \frac{v}{c}\cos\left(\theta_{k,l,n}\right)\right)\cos\left(\theta_{k,l,n}\right). \tag{4}$$

In practice, BSs are distributed along the rail, each of which provides service in a specific area. We mainly consider the communication in a cell and the range of $\theta_{k,l,n}$ is much smaller than $(0, \pi)$. Under this condition, (4) can be rewritten as $s_{l,n} = \frac{d}{\lambda}\cos(\theta'_{k,l,n})$, where $\theta'_{k,n}$ is the actual AOA of signal. For easy reference, details about variables are given in Table I.

III. JOINT COMPENSATION FOR DOPPLER SHIFT AND BEAM ALIGNMENT

In the HSR scenario, the DFO caused by high-speed moving terminals introduces great challenges for receiving signals. One of the challenges is that the absolute DFO ($\phi_{f_{D,l,n}}$) results in extra carrier frequency synchronization error and thus worsens ICI [16]. According to the expression of absolute DFO, $\phi_{f_{D,l,n}}$ is positively correlated with train speed, v. Increasing v will lead to larger phase error for signal reception and worsen both the training error and bit error rate (BER). Another challenge is the difficulty to compensate for DFO since for a multipath channel, each path has a unique AOA and corresponding relative Doppler shift ($\mathbf{b}_{k,l,n}$)[38]. Only the transmitter equipped with a large-scale antenna array can distinguish multiple DFOs [39], which means that in uplink, single-antenna TEs cannot precompensate for DFO.

A natural question is how to compensate for the DFO in uplink? By investigating the spatial characteristics of the HSR channel [14], [20]–[22], we propose a joint DFO compensation and AOA estimation scheme. The key idea is capturing the exact AOA information of the LoS path and using nonorthogonal angular beamforming to compensate for DFO directly. To introduce the scheme more clearly, we first discuss the spatial characteristics of the channel.

In (1), the relative DFO matrix acts as the phase rotation matrix, which induces an angular shift of the AOA. An 512-point DFT of the channel is shown in Fig. 2. The blue lines in the figure denote the orthogonal beams when the train is in the rest state [35, Part A, Sec IV]. The beam index with the maximum value reflects the rough information of AOA. The angle of the aligned beam is the same as the TE azimuth angle, i.e., $\theta_{k,n}$. In the high-speed moving process, relative DFO leads to an angular shift of the aligned beam from the *Y*-axis to the green line, which corresponds to the actual AOA of the signal, i.e., $\theta'_{k,n}$ ($\theta'_{k,n} < \theta_{k,n}$). For each path, the relationship between $\theta_{k,n}$ and $\theta'_{k,n}$ is given in (4). It shows that $\theta'_{k,n}$ is negatively correlated with train speed, increasing v will lead to decrease of $\theta'_{k,n}$. In other words, the angular error is increased.[4] Note that absolute DFO does not influence the spatial property of the channel because each of the antenna elements suffers from the same $\phi_{f_{D,l,n}}$, which is different from relative DFO.

Since both absolute and relative DFO are related to the AOA of signals, a specific method should be applied to capture accurate

[4]In practice, the angular shift from $\theta_{k,n}$ to $\theta'_{k,n}$ is small since v is much smaller than the speed of light, c The approximation, $\theta'_{k,n} \approx \theta_{k,n}$ is precise when the accuracy is retained to 3 digits after the decimal point. However, ULA is sensitive to angle error. Whether the angular difference between $\theta_{k,n}$ and $\theta'_{k,n}$ can be distinguished depends on antennas number and oversampling factor as will be mentioned later on. To keep the rigor of derivation, $\theta'_{k,n}$ is considered.

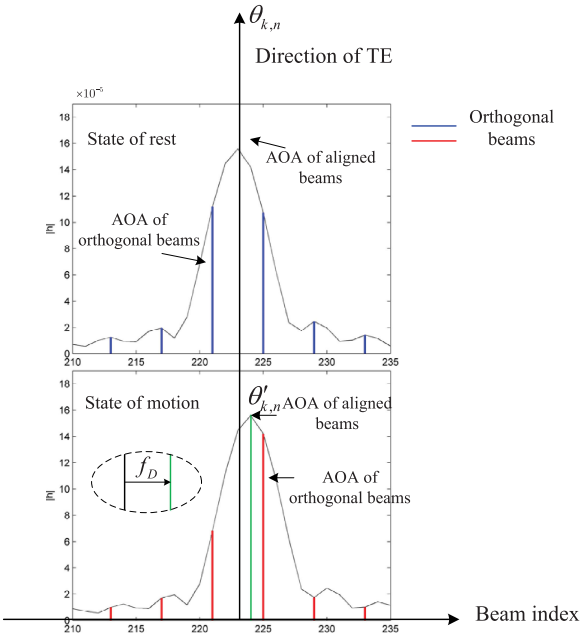

Fig. 2. Illustration of the 512-point DFT of channel with AS in $[20°, 40°]$. The azimuth angle is $\theta_{k,n} = 30°$, whose beam index is 223.

AOA information. Here, we present a simplified digital approach to realize beam alignment and AOA estimation.

Explicitly, the pilot signal received from the kth TE is expressed as

$$\mathbf{y}_{k,n} = \mathbf{h}_{k,n,f_D}\mathbf{x}_k + \mathbf{n}_{\mathbf{k,n}} \tag{5}$$

where $\mathbf{x_k} \in \mathbb{C}^{1\times\tau}$ is the pilot signal and $(\tau \geq K)$. p_τ is the mean power of each pilot signal. $\mathbf{n}_{k,n} \in \mathbb{C}^{M\times\tau}$ is the zero-mean additive Gaussian white noise, the elements of which comply with $\mathcal{CN}(0, \sigma_n^2)$. Let $\hat{\mathbf{h}}_{k,n,f_D} \in \mathbb{C}^{M\times 1}$ denote the initial estimation of the channel by using typical methods such as minimum mean square error (MMSE) and least squares (LS).

$$\mathbf{F} = \frac{1}{\sqrt{M}}\begin{bmatrix} 1 & 1 & \cdots & 1 \\ 1 & e^{-j2\pi\Delta f} & \cdots & e^{-j2\pi(M-1)\Delta f} \\ \vdots & \vdots & \vdots & \vdots \\ 1 & e^{-j2\pi(M-1)\Delta f} & \cdots & e^{-j2\pi(M-1)^2\Delta f} \end{bmatrix} \tag{6}$$

is the normalized DFT matrix, where $\Delta f = \frac{1}{M}$ is the spatial resolution of the ULA. Then, M-point DFT of the estimated channel can be expressed as $\tilde{\mathbf{h}}_{k,n,f_D} = \mathbf{F}\hat{\mathbf{h}}_{k,n,f_D}$. Since each column of $\mathbf{F}$ acts as a beam toward the physical direction, the modulus of elements in $\tilde{\mathbf{h}}_{k,n,f_D}$ reflects the distribution of gain in all directions. All of the beams are orthogonal, which forms an orthogonal beamspace (OBS), and only a small number of beams are significant, which point to the direction of the signal [40, Part B, Sec II]. However, due to the use of the DFT matrix, the OBS scheme relies on fixed-direction beams toward the equally spaced AOA, and the spatial resolution is only Δf. If the AOA of the signal is not an integer multiple of Δf, power leakage will occur [35, Part B, Sec. IV], which will lead to a wider AS.

Fig. 3 depicts the power distribution of $\tilde{\mathbf{h}}_{k,n,f_D} \in \mathbb{C}^{M\times 1}$ with 20 paths, which has the same channel parameters with that in the lower half of Fig. 2, $\theta_{k,n} = 30°$, the AS is 20°. As the same with Fig. 2, the red lines denote orthogonal beams. Since $\theta_{k,n}$ is not an integer multiple of Δf, the power leakage happens. Over 95

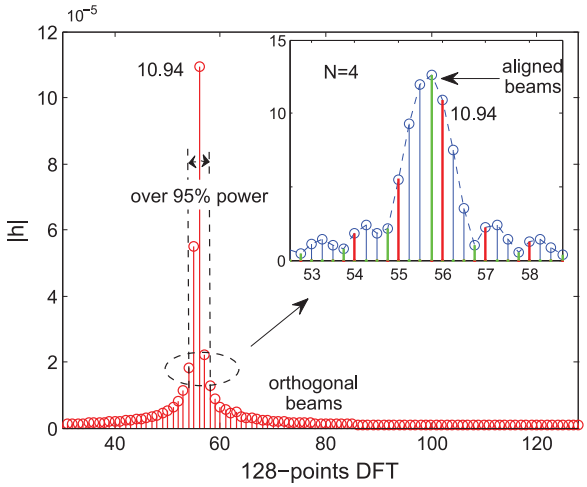

Fig. 3. Illustration of the 128-point DFT of channel with angle spread in $[20°, 40°]$, $M = 128$, the azimuth angle is $\theta_{k,n} = 30°$.

percent of the power concentrates on five red beams, whose index are from 54 to 59. The beam with maximal value points to the direction of 30.75°. The aligned beams are shown as green lines in the inset. Since the beam with maximal value occupies over 90 percent of power, power leakage is well suppressed. A general solution for aligning beams and suppressing beam spread is to search for the optimal phase rotation matrix to enhance the resolution of the antenna array and sample the peak value of channel gain. In [26], [40], a one-dimensional search is performed to acquire the optimal rotation angle. In [35], a digital approach is designed by padding zeros at the end of the channel vector and performing DFT. Note that neither of these approaches are suitable for the HSR scenario because digital realization of the former is difficult, while the latter further increases the computational complexity of high-dimensional channels. Inspired by these approaches, we present a simplified digital realization scheme that only uses local FFT oversampling and has low complexity. Denote

$$\mathbf{O}\left(\phi_{k,n,u}\right) = diag\left(1, e^{j\phi_{k,n,u}}, \ldots, e^{j(M-1)\phi_{k,n,u}}\right) \tag{7}$$

where $\phi_{k,n,u}$ is the rotation angle and $-\frac{\pi}{M} \leq \phi_{k,n,u} \leq \frac{\pi}{M}$. Then, the modified DFT of the estimated channel is expressed as

$$\tilde{\mathbf{h}}^r_{k,n,f_D} = \mathbf{FO}\left(\phi_{k,n,u}\right)\hat{\mathbf{h}}_{k,n,f_D} = \sum_{l=1}^{L} e^{j\left(\phi_n + \phi_{f_D,l,n}\right)} \cdot \psi_l \alpha_{k,l,n}\mathbf{FO}\left(\phi_{k,n,u}\right)\mathbf{O}\left(f_{D,l,n}\right)\mathbf{a}\left(\theta_{k,l,n}\right). \tag{8}$$

Here, we need to find the optimal $\phi^0_{k,n,u}$ that satisfies

$$\phi^0_{k,n,u} = \arg\max_{\phi_{k,n,u}} \tilde{\mathbf{h}}^{r\max}_{k,n,f_D} \tag{9}$$

where $\tilde{\mathbf{h}}^{r\max}_{k,n,f_D}$ is the maximum value of $|\tilde{\mathbf{h}}^r_{k,n,f_D}|$. Define $\tilde{\mathbf{g}}_{k,n,f_D} \in \mathbb{C}^{MN\times 1}$ as the NM-point FFT of $\hat{\mathbf{h}}_{k,n,f_D}$, where N is the number of oversamplings. The relationship between the oversampling signal and the initial M-point DFT signal is

$$\left(\tilde{\mathbf{h}}_{k,n,f_D}\right)_m = \left(\tilde{\mathbf{g}}_{k,n,f_D}\right)_{(m-1)N+1}, (1 \leq m \leq M). \tag{10}$$

Let i_k denote the beam index with maximum power; then, the maximum value of $\tilde{\mathbf{h}}_{k,n,f_D}$ can be expressed as

$$\left(\tilde{\mathbf{h}}_{k,n,f_D}\right)_{i_k} = \left(\tilde{\mathbf{g}}_{k,n,f_D}\right)_{(i_k-1)N+1}. \tag{11}$$

Here, we focus on the FFT point region in $[(i_k-2)N+1,\ i_kN+1]$, in which three orthogonal beams are moved through N possible steps to search for the optimal step n. Note that the region of n should be classified according to the odd–even property of N. The relationship is given as

$$n \in \begin{cases} \left(-\frac{N}{2}, \frac{N}{2}\right], & N \text{ is even} \\ \left(-\frac{N-1}{2}, \frac{N+1}{2}\right], & N \text{ is odd.} \end{cases} \tag{12}$$

By calculating $2N$ point oversampling, the optimal rotation angle is given as

$$\phi^0_{k,n,u} = \frac{n}{N} 2\pi \Delta f \tag{13}$$

$$\begin{aligned} \left(\tilde{\mathbf{h}}^r_{k,n,f_D}\right)_i &= e^{j\left(\phi_n+\phi_{f_D,l,n}\right)} \sum_{l=1}^{L} \frac{\psi_l \alpha_{k,l,n}}{\sqrt{M}} \\ &\times \left(1 + e^{-j\left[\frac{2\pi(i-1)}{M} - (2\pi s_{l,n}+\phi_{k,l,n})\right]}\right. \\ &\left. + \cdots + e^{-j(M-1)\left[\frac{2\pi(i-1)}{M} - (2\pi s_{l,n}+\phi_{k,l,n})\right]}\right) \\ &= e^{j\left(\phi_n+\phi_{f_D,l,n}\right)} \sum_{l=1}^{L} \sum_{m=0}^{M-1} \frac{\psi_l \alpha_{k,l,n}}{\sqrt{M}} e^{-jm\left[\frac{2\pi(i-1)}{M} - (2\pi s_{l,n}+\phi_{k,l,n})\right]} \\ &= e^{j\left(\phi_n+\phi_{f_D,l,n}\right)} \sum_{l=1}^{L} \frac{\psi_l \alpha_{k,l,n}}{\sqrt{M}} e^{-j\frac{M-1}{2}\left[\frac{2\pi(i-1)}{M}\right.} \\ &\left. - (2\pi s_{l,n}+\phi_{k,l,n})\right] \frac{\sin\left\{\left[\frac{2\pi(i-1)}{M} - 2\pi s_{l,n} - \phi_{k,l,n}\right]\frac{M}{2}\right\}}{\sin\left\{\left[\frac{2\pi(i-1)}{M} - 2\pi s_{l,n} - \phi_{k,l,n}\right]\frac{1}{2}\right\}}. \end{aligned} \tag{14}$$

From (8), the ith element of $\tilde{\mathbf{h}}^r_{k,n,f_D}$ is expressed as (14). According to (14), the value of $\tilde{\mathbf{h}}^r_{k,n,f_D}$ is determined by gains from all the paths. In the case of single path channel, the expression is in the form of aliased sine function, according to the envelop of the squared aliased sine function [34], when $\frac{2\pi(i-1)}{M} - 2\pi s - \phi_{k,l,n} = 0$ in (14) is satisfied, the modulus of function obtains the maximal value, i.e., the ith beam points toward the aligned direction and thus obtains the largest channel gain. For the case of multipath channels, since the Rician factor is very large in viaduct and cutting scenarios [30], meanwhile AS is relatively small [20]–[22], i.e., scattering paths are distributed near LoS path, the optimal rotation angle of multipath channel is nearly equal to the optimal rotation angle for the LoS path, i.e., $\phi^0_{k,n,u} = \phi^0_{k,1,n,u}$

$$\frac{2\pi\left(i_k-1\right)}{M} - 2\pi s_{1,n} - \phi^0_{k,n,u} = 0. \tag{15}$$

When $\phi^0_{k,n,u}$ is obtained from FFT oversampling and the beam index of the largest gain is acquired, by substituting these two parameters into (15), $s_{1,n}$ can be obtained. Combined with (4), both $\theta_{k,n}$ and $\theta'_{k,n}$ can be calculated.

By using the phase rotation matrix and aligning beams, the modified power distribution is shown as green lines in Fig. 3. As shown, the beam spread is significantly suppressed, and most of the power concentrates on one beam. Except for AOA, the Doppler shift in the LoS path is also decided by the velocity and wavelength. The former can be acquired from the communication-based train control system [41], while the latter can easily be obtained from the carrier frequency. Then, the Doppler shift in the LoS path can be calculated. In practice, it is difficult to estimate the DFO in NLoS paths because the BS receives the overlap of multipath signals; meanwhile, in viaduct and cutting scenarios, the Rician factor is greater than 20 dB, and the power of NLoS paths is rather small [20]. Thus, the main idea of compensating for DFO in uplink is performing beam alignment to receive signals from the actual AOA in the LoS path ($\theta'_{k,1,n}$). The DFO compensation matrix in uplink is given as

$$\begin{aligned} \mathbf{W}_{f_D,n,u} &= \mathbf{B}_{n,u}\mathbf{\Phi}_{n,u} \\ \mathbf{\Phi}_{n,u} &= \text{diag}\left(e^{j\phi_{f_{D_1},1,n}}, \ldots, e^{j\phi_{f_{D_K},1,n}}\right) \\ \mathbf{B}_{n,u} &= \left[\mathbf{O}^H\left(\phi^0_{1,n,u}\right)\mathbf{f}^*_{i_1}, \ldots, \mathbf{O}^H\left(\phi^0_{K,n,u}\right)\mathbf{f}^*_{i_K}\right] \end{aligned} \tag{16}$$

where $\mathbf{\Phi}_{n,u} \in \mathbb{C}^{K\times K}$ denotes the absolute DFO compensation matrix. $\mathbf{B}_{n,u} \in \mathbb{C}^{M\times K}$ denotes the angular beamforming matrix, and $\mathbf{f}^*_{i_k} \in \mathbb{C}^{M\times 1}$ denotes the conjugate of the i_kth column in $\mathbf{F}$. Details about the derivation of $\mathbf{B}_{n,u}$ will be presented in Section IV.

In downlink, the DFO compensation is different from that in uplink. Precompensation is performed to transmit signals toward the azimuth angle of TEs ($\theta_{k,1,n}$). The DFO compensation matrix is given as

$$\begin{aligned} \mathbf{W}_{f_D,n,d} &= \mathbf{B}_{n,d}\Phi_{n,d} \\ \mathbf{B}_{n,d} &= \begin{bmatrix} \mathbf{f}^T_{i_1}\mathbf{O}\left(\phi^0_{1,n,d}\right)\mathbf{O}^{-1}\left(f_{D_1,1,n}\right) \\ \vdots \\ \mathbf{f}^T_{i_K}\mathbf{O}\left(\phi^0_{K,n,d}\right)\mathbf{O}^{-1}\left(f_{D_K,1,n}\right) \end{bmatrix}^H \\ \mathbf{\Phi}_{n,d} &= \mathbf{\Phi}_{n,u}. \end{aligned} \tag{17}$$

IV. Angle-Domain Channel Tracking Scheme

Traditional mobile communication systems are designed for users who are stationary or moving at low speed, whereas in the HSR scenario, the high mobility of the train shortens the length of the CT and thus causes more frequent channel estimation, which deteriorates the SE and increases the burden on the BS. To reduce the training overhead, a joint spatial–temporal-correlation-based channel estimation scheme was proposed in [10], and a time-varying spatial-correlation-based KF scheme was proposed in [12]. An extended KF (EKF)-based AOA tracking scheme was introduced in [29]. An AD channel tracking scheme that utilizes a UKF to track spatial angular information was presented in [26] and [27].

One problem for the proposed schemes is that in the HSR scenario, the vulnerability of the doubly selective fading channel is not considered. The motion of a train in a CT may lead to a change in scattering paths and corresponding shadow fading, which makes the estimated CSI during the first few slots unreliable. In addition, extra phase error causing from nonnegligible DFO decreases the accuracy of CSI acquisition. Another problem is the pilot overhead is relatively high. Hence, from a practical perspective, we propose a KF-based channel tracking scheme. The channel tracking scheme is implemented in angle-domain, in which the FD channel is decomposed into AOA information and beam gain. The linear KF is used to modify the measured beam gain according to the MMSE principle. The proposed tracking scheme is robust and self-adaptive to channel conditions, meanwhile the pilot overhead and computational complexity is significantly reduced.[5] Note that the tracked CSI still includes the relative DFO, and the original CSI without Doppler shift can be acquired by left multiplying $\mathbf{O}^{-1}(f_{D,1,n})$. Based on the reciprocity in TDD systems, the downlink CSI can be acquired immediately. Since DFO has been compensated and the phase of the carrier frequency is well estimated from synchronization, during the overall process of introducing the tracking scheme, the subscript f_D in $\mathbf{h}_{k,n,f_D}$ is removed, and the phase of the carrier frequency is not considered. The channel model from (3) is refined as

$$\mathbf{h}_{k,n} = \sum_{l=1}^{L} \psi_l \alpha_{k,l,n} \mathbf{a}\left(\theta'_{k,l,n}\right). \tag{18}$$

The spatial angular property of the HSR channel was discussed in Section III; here, we introduce the temporal property. The relationship of AOA between adjacent CTs can be expressed as

$$\theta'_{k,l,n+1} = \theta'_{k,l,n} + \Delta\theta'_{k,l,n} \tag{19}$$

where $\Delta\theta'_{k,l,n}$ denotes the variation of AOA in a CT. Although the spatial resolution of ULA is enhanced, the antenna array is insensitive to slight changes in spatial angular information in a few CTs because the variation in AOA does not reach the maximum resolution. Define the AOA time (AOAT) as the duration when the accumulated variance of AOA is less than Δf[6]

$$\begin{aligned} &\text{AOAT} = \max N_m \\ &\text{s.t.} \sum_{n=1}^{N} \Delta\theta_{k,l,n} \le \frac{\Delta f}{N}. \end{aligned} \tag{20}$$

Since rails are fixed on one side of BS, the region of AOA is defined as (θ_1, θ_2), where $0 < \theta_1 < \theta_2 < \pi$. The geometrical relationship between BS and TEs is shown in Fig. 4. For simplifying the mathematical model, the relative heights of the BS and train are not considered. Define d_m as the initial horizontal distance from the kth TE to the BS in the mth CT, d_0 is the vertical distance between the BS and rail. When train moves close to BS, $\theta'_{k,1,n} \in (\theta_1, \frac{\pi}{2}]$, based on the trigonometric relationship

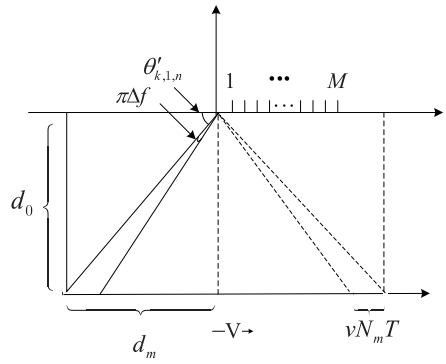

Fig. 4. Geometrical relationship between BS and TEs.

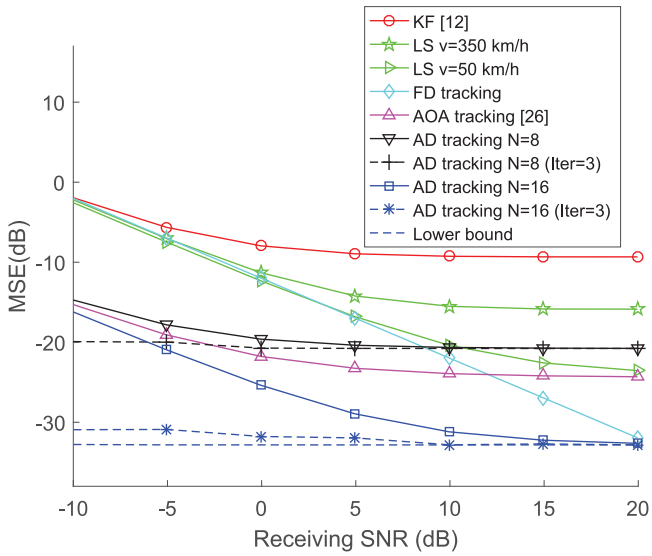

Fig. 5. MSE of angle-domain channel tracking scheme. $\theta_{k,1,n} = 30°$, and the AS is $[20°, 40°]$. The oversampling factor is $N = 8, 16$, the iteration number of AD tracking scheme is $Iter = 1, 3$. $v = 350$ km/h

in Fig. 4, we have $\tan(\theta'_{k,1,n} + \pi\Delta f) = d_0/(d_m - vN_mT)$. Similarly, we have $\tan(\pi - \theta - \pi\Delta f) = d_0/(d_m + vN_mT)$ when train moves away from BS. Based on these two equations, the length of the mth AOAT is given as follows:

$$N_m = \begin{cases} \frac{1}{vT}\left(d_m - \frac{d_0}{\tan(\theta'_{k,1,n}+\pi\Delta f)}\right), \theta'_{k,1,n} \in \left(\theta_1, \frac{\pi}{2}\right] \\ \frac{1}{vT}\left(\frac{d_0}{\tan(\pi-\theta'_{k,1,n}-\pi\Delta f)} - d_m\right), \theta'_{k,1,n} \in \left(\frac{\pi}{2}, \theta_2\right) \end{cases}. \tag{21}$$

Thus, only when CT n and CT $n+1$ are in different AOATs does $\Delta\theta'_{k,l,n} \neq 0°$. Otherwise, the variation in AOA can be approximated as zero.

According to the temporal coherence, the array response gain is rewritten as

$$\alpha_{k,l,n+1} = \rho_l \alpha_{k,l,n} + \sqrt{1-\rho^2}\beta_{k,l,n} \tag{22}$$

where ρ_l is the temporal correlation coefficient, which depicts the variance of time correlation during adjacent CTs. $\beta_{k,l,n}$ is a random variable that is independent and identically distributed (i.i.d.) with $\alpha_{k,l,n}$, i.e., $\beta_{k,l,n} \sim \mathcal{CN}(0, \sigma^2_{k,l,n})$. For a high-Rician channel, NLoS paths are nonuniformly distributed around train, the temporal correlation coefficient is different for

[5]The angle-domain channel tracking scheme aims to track time-varying CSI, which is based on the pre-estimated AOA and pilot signals. Thus, no other additional reference signals are needed.

[6]The spatial resolution is determined by antenna number M and oversampling times N. Considering the cost and system complexity, M is limited. Thus, the length of AOAT is mainly determined by N. A tradeoff should be made between AOAT and N to guarantee both the array resolution and tracking period.

LoS and NLoS paths. According to space-time correlation function under nonisotropic scattering environment [42, Eq. (12)], the temporal correlation coefficient of the NLoS component is expressed as

$$\rho_l = \frac{I_0\left(\sqrt{\kappa^2 - 4\pi^2 f_D^2 T^2 + j4\pi\kappa\cos(\mu) f_D T}\right)}{I_0(\kappa)},\ l \geq 2 \quad (23)$$

where $I_0(\cdot)$ is the zeroth-order modified Bessel function, $\kappa > 0$ is a factor which controls the width of AOA of scatter components. For a unidirectional scattering scenario (large κ), the width of AOA is roughly equal to $2/\sqrt{\kappa}$ [43]. f_D is the maximal Doppler shift, μ accounts for the mean direction of AOA. Assume that scattering paths are distributed near LoS path, then we have $\mu \approx \theta'_{k,1,n}$. In [42], the discussion about space-time correlation of LoS component is given in Part. B, Section III. Since each TE is equipped with a single antenna, the space-time cross-correlation function [42, Eq.(18)] can be simplified as temporal correlation model, which is expressed as

$$\rho_l = \frac{\mathcal{K}}{\mathcal{K}+1}\exp\left[j2\pi f_D T\cos(\gamma) + j\frac{2\pi d}{\lambda}\cos(\alpha)\right],\ l = 1 \quad (24)$$

where γ is the relative moving direction between the train and BS. In the case of moving across the region covered by BS, generally we set $\gamma = 180^\circ$. α is the layout angle of ULA, which is set to be 0°.

From (23) and (24) we can see that the temporal correlation coefficient for LoS component is a constant, which is mainly determined by the Rician factor, while the coefficient for the NLoS component is a function of μ. Based on the measurement of Rician-factor in viaduct and U-shape cutting scenarios [30], κ is large, the value of ρ_1 is very close to one ($0.95 < |\rho_1| < 1$), which shows good fit to the results in [44]. According to the measurement of AS [21], the mean AS in the HSR scenario is 30°, i.e., $\kappa = 15$. For $\mu \in (0, \pi)$, the temporal correlation coefficient of NLoS component has a minimum value, 0.9, when $\mu = 90^\circ$. Thus both the LoS and NLoS paths obtain high temporal correlation. For the convenience of simplifying formula derivation, we make a approximation, i.e., $\rho_l = \rho, l \geq 1$.

Substituting (22) and (24) into (18), the multipath channel in CT $n+1$ is expressed as

$$\begin{aligned}\mathbf{h}_{k,n+1} &= \sum_{l=1}^{L}\psi_l\alpha_{k,l,n+1}\mathbf{a}\left(\theta'_{k,l,n+1}\right)\\ &= \sum_{l=1}^{L}\left(\rho\mathbf{T}_{k,l,n}\mathbf{h}_{k,l,n} + \sqrt{1-\rho^2}\mathbf{c}_{k,l,n+1}\right)\end{aligned} \quad (25)$$

where $\mathbf{T}_{k,l,n} \in \mathbb{C}^{M\times M}$ and $\mathbf{c}_{k,l,n+1} \in \mathbb{C}^{M\times 1}$ are written as

$$\mathbf{T}_{k,l,n} = \mathrm{diag}\left(1, \ldots, e^{j\frac{2\pi(M-1)d}{\lambda}\left(\cos\left(\theta'_{k,l,n+1}\right) - \cos\left(\theta'_{k,l,n}\right)\right)}\right) \quad (26)$$

$$\mathbf{c}_{k,l,n+1} = \psi_l\beta_{k,l,n+1}\mathbf{T}_{k,l,n}\mathbf{a}\left(\theta'_{k,l,n}\right). \quad (27)$$

According to the above discussion, $\Delta\theta'_{k,l,n} \neq 0^\circ$ occurs only when adjacent CTs belong to different AOATs. Here, we first consider the condition in which TEs are served by invariant beams, i.e., $\Delta\theta'_{k,l,n} = 0^\circ$. By substituting (19), (26), and (27) into (25), the multipath channel in CT $n+1$ is rewritten as

$$\mathbf{h}_{k,n+1} = \rho\mathbf{h}_{k,n} + \sqrt{1-\rho^2}\mathbf{c}_{k,n+1} \quad (28)$$

where $\mathbf{c}_{k,n+1}$ is given as $\mathbf{c}_{k,n+1} = \sum_{l=1}^{L}\psi_l\beta_{k,l,n+1}\mathbf{a}(\theta'_{k,l,n}) \cong \mathbf{h}_{k,n}$., "$\cong$" means equality in probabilistic distribution. The received pilot signal in (5) is rewritten as

$$\begin{aligned}\mathbf{y}'_{k,n+1} &= \mathbf{y}_{k,n+1}\mathbf{x}_k^H\\ &= \tau p_\tau\mathbf{h}_{k,n+1} + \mathbf{n}_{k,n+1}\mathbf{x}_k^H.\end{aligned} \quad (29)$$

According to (13), the optimal rotation angle $\phi^0_{k,n,u}$ is obtained. Based on (13), (18), and strong Rician property, a valid approximation of $\mathbf{h}_{k,n}$ with one beam vector can be expressed as

$$\begin{aligned}\mathbf{h}_{k,n} &= \mathbf{O}^H\left(\phi^0_{k,n,u}\right)\mathbf{F}^H\tilde{\mathbf{h}}^{r_0}_{k,n}\\ &\approx \left(\tilde{\mathbf{h}}^{r_0}_{k,n}\right)_{i_k}\mathbf{O}^H\left(\phi^0_{k,n,u}\right)\mathbf{f}^*_{i_k}.\end{aligned} \quad (30)$$

Then the BD channel $\tilde{\mathbf{H}}^{\{B_{r_0}\}}_{n,f_D} \in \mathbb{C}^{K\times K}$ is expressed as

$$\tilde{\mathbf{H}}^{\{B_{r_0}\}}_{n} = \mathbf{B}^H\mathbf{H}_n \quad (31)$$

where $\{B^{r_0}\}$ is the beam set which contains K aligned beams. Comparing with $\mathbf{H}_n \in \mathbb{C}^{M\times K}$, $\tilde{\mathbf{H}}^{\{B_{r_0}\}}_n$ is a K-order square matrix, the dimension of BD channel is decreased from M to K.

From (30) we can find that the FD channel is composed of angular information vector, $\mathbf{O}^H(\phi^0_{k,n,u})\mathbf{f}^*_{i_k}$, and one-dimensional beam gain value, $(\tilde{\mathbf{h}}^{r_0}_{k,n})_{i_k}$. Since angular information is invariant during the tracking period and can be acquired at the beginning of AOAT, the main target of angle-domain channel tracking scheme is tracing $(\tilde{\mathbf{h}}^{r_0}_{k,n})_{i_k}$ so as to reconstruct full dimension channel from (30) and acquire BD channel from (31).

By multiplying $\mathbf{f}^T_{i_k}\mathbf{O}(\phi^0_{k,n,u})$ on both sides of (28) and (29), the angle domain state space is given as

$$\left(\tilde{\mathbf{h}}^{r_0}_{k,n+1}\right)_{i_k} = \rho\left(\tilde{\mathbf{h}}^{r_0}_{k,n}\right)_{i_k} + \sqrt{1-\rho^2}\left(\tilde{\mathbf{c}}^{r_0}_{k,n+1}\right)_{i_k} \quad (32)$$

$$\tilde{\mathbf{y}}'^{r_0}_{k,n+1} = \tau p_\tau\left(\tilde{\mathbf{h}}^{r_0}_{k,n+1}\right)_{i_k} + \left(\tilde{\mathbf{n}}^{r_0}_{k,n+1}\right)_{i_k}\mathbf{x}^H_{k,n+1}. \quad (33)$$

Based on the angle domain state space and the structure of KF [45], [46], the equation series of tracking are given from (34) to (38), where $p_{k,n+1|n}$ is the prediction of angle domain beam gain error, $p_{k,n+1|n} = \mathbb{E}\{[(\tilde{h}^{r_0}_{k,n})_{i_k} - (\tilde{h}^{r_0}_{k,n+1|n})_{i_k}]^2\}$. $\mathbf{R}_{k,n} = \mathbb{E}\{\mathbf{h}_{k,n}\mathbf{h}^H_{k,n}\}$ is the channel covariance matrix, kg is the Kalman factor, $p_{k,n+1|n+1}$ is the optimal estimation of error. Equations (34) and (35) are the prediction of channel and estimation error, which is blind and only depend on the CSI of last CT. Equations (36) and (38) are the modification of (34) and (35) respectively, which depend on both the prediction and measurement.

$$\left(\tilde{\mathbf{h}}^{r_0}_{k,n+1|n}\right)_{i_k} = \rho\left(\tilde{\mathbf{h}}^{r_0}_{k,n|n}\right)_{i_k} \quad (34)$$

$$p_{k,n+1|n} = \rho^2 p_{k,n|n} + (1-\rho^2)\mathbf{f}^T_{i_k}\mathbf{O}\left(\phi^0_{k,n,u}\right)\mathbf{R}_{k,n}\mathbf{O}^H\left(\phi^0_{k,n,u}\right)\mathbf{f}^*_{i_k} \quad (35)$$

$$\left(\tilde{\mathbf{h}}^{r_0}_{k,n+1|n+1}\right)_{i_k} = \left(\tilde{\mathbf{h}}^{r_0}_{k,n+1|n}\right)_{i_k} + kg\left(\tilde{\mathbf{y}}'^{r_0}_{k,n+1} - \tau p_\tau\left(\tilde{\mathbf{h}}^{r_0}_{k,n+1|n}\right)_{i_k}\right) \quad (36)$$

$$kg = \frac{p_{k,n+1|n}}{\tau p_\tau p_{k,n+1|n} + \sigma_n^2} \quad (37)$$

$$p_{k,n+1|n+1} = (1 - kg\tau p_\tau)\, p_{k,n+1|n} \quad (38)$$

Algorithm 1: TE Grouping and Pilot Reuse Scheme.

1. Initialization:
1) Calculate $\tilde{\mathbf{h}}_{k,n}^{r_0}$ from (8) and (13). Acquire active beam set $B_{k,a}$ that contains over η percent of power.
2) Number TEs in consecutive order. Define G and C_g as the number of groups and TE set of the gth group, respectively. $C_g = \emptyset, 1 \le g \le G$. $rem(\cdot)$ is the remainder operator.

2. for $k = 2 : K$
  if $B_{k,a} \cap B_{1,a} = \emptyset$
    return $G = k - 1$;
    break;
  end if
end for
for $k = 1 : K$
  for $g = 1 : G$
    if $rem(k - g, G) = 0$
      $C_g = C_g \cup \{k\}$;
    end if
  end for
  end for

3. Each of the groups use different pilot signals, while TEs in the same group use the same pilot signal, whose length is $\tau = G$.

Algorithm 2: Angle-Domain Channel Tracking Scheme.

1. Initialization:
1) Define

$$\Delta\gamma_{k,n+1} = \gamma_{k,n+1} - \gamma_{k,n}$$

as the variation in the uplink receiving SINR. Define v_t as the threshold of SINR change.
2) Calculate the mth AOAT that includes N_m CTs.

2. while AOAT index $= m$ **do**
1) Acquire $\hat{\mathbf{h}}_{k,1|1}$ and $\tilde{\mathbf{h}}_{k,1|1}$. $p_{k,1|1} = 0$.
2) Use (11) and (13) to calculate $\left(\tilde{\mathbf{h}}_{k,1|1}^{r_0}\right)_{i_k}$, $\phi_{k,1,1}^0$ and $\mathbf{f}_{i_k}$, respectively. $\phi_{k,1,n}^0 = \phi_{k,1,1}^0$.
3) Group TE according to **Algorithm 2**. Set the length of the pilot sequence.

  for $n = 2, \ldots, N_m$
    Calculate $\left(\tilde{\mathbf{h}}_{k,n|n}^{r_0}\right)_{i_k}$ with (36) and renew $p_{k,n|n}$ with (38). Monitor $\Delta\gamma_{k,n}$.
    if $\Delta\gamma_{k,n} > v_t$
      Ask for extra pilot frame through control channel. Modify $\left(\tilde{\mathbf{h}}_{k,n|n}^{r_0}\right)_{i_k}$ with (36). Modify $p_{k,n|n}$ with (38).
    end if
  end for
end while

When the train is tracked in the same period, the AOA of channel is invariant. At the beginning of each CT, equation (36) is used to modify the CSI according to the principle of MMSE. During the CT, the channel estimation error is monitored according to the abrupt change in the instantaneous signal-to-interference-plus-noise-ratio (SINR). If no change occurs in the CSI, the initial modified CSI will be considered invariant during the whole CT (case 1). Otherwise, an extra pilot frame will be inserted into the data frame queue to renew the CSI (case 2).

When the train is served in a new AOAT, the renewal of angular information will lead to a new period of tracking, during which normal CSI acquisition should be performed at the beginning to acquire spatial angular information and compensate for DFO. In practice, some of the HSR scenarios have no obvious Rician factor, such as deep U-shape cutting and urban. The estimation error will be increased by applying AD tracking scheme. However, the method can be easily extended to BD, which is suitable for tracking the Rayleigh channel, because the FD state space is the same with (28) and (29). Thus the proposed tracking method can be applied to other scenarios.

Another problem that we consider is how to reduce the pilot overhead in the channel modification part. In the HSR scenario, the CT is shortened, and the training process will compress the residual time slots for data transmission. However, for guaranteeing the orthogonality of pilot signals, the length of the pilot signals τ should satisfy $\tau \ge K$ [31]. Fortunately, by utilizing the high angular resolution from ULA, user grouping and pilot reuse method can be applied to significantly reduce the pilot overhead. As discussed in Section III, the gains of different channels are clearly distinguished by spatial angular information. By using beam alignment, the power leakage is well suppressed and poses small interference to adjacent channels. The TE grouping and pilot reuse scheme is introduced in Algorithm 1. Then, the AD channel tracking scheme is presented in Algorithm 2. From these two algorithms we can see that one-dimensional beam gain value is tracked by applying temporal correlation between adjacent CTs, compared with M-dimensional channel matrix, the computational complexity is well reduced. Meanwhile TEs grouping and pilot reuse scheme is applied to significantly reduce the pilot overhead from TEs' number to group number.

V. Angle-Domain Uplink/Downlink Transmission

In this section, we propose an AD transmission scheme. The hybrid beamforming is composed of three parts: DFO compensation, angular beamforming, and BD reception/precoding. In practice, the DFO compensation can be realized by modifying the phase. The angular beamforming is realized by using phase shifters in the analog domain, while the BD reception/precoding can be implemented in the digital domain because the size is much smaller. Define $\mathbf{P}_{n,u} \in \mathbb{C}^{K \times K}$ as the BD reception matrix. We use zero forcing (ZF) to eliminate multiuser interference.

$$\mathbf{P}_{n,u} = \tilde{\mathbf{H}}_n^{\{B_{r0}\}} \left[\left(\tilde{\mathbf{H}}_n^{\{B_{r0}\}} \right)^H \tilde{\mathbf{H}}_n^{\{B_{r0}\}} \right]^{-1}. \tag{39}$$

Based on (16) and (39), the uplink hybrid beamforming matrix is expressed as

$$\mathbf{W}_{n,u} = \mathbf{B}_{n,u} \Phi_{n,u} \mathbf{P}_{n,u}. \tag{40}$$

Then, the uplink received signal is expressed as

$$\begin{aligned}\tilde{\mathbf{y}}_{n,u} &= \mathbf{W}_{n,u}^H \mathbf{H}_{n,f_D} \mathbf{x}_u + \mathbf{W}_{n,u}^H \mathbf{n}_u \\ &= \mathbf{P}_{n,u}^H \tilde{\mathbf{H}}_n^{\{B_{r_0}\}} \mathbf{x}_u + \mathbf{P}_{n,u}^H \tilde{\mathbf{n}}_u^{\{B_{r_0}\}}. \end{aligned} \tag{41}$$

From (41), the BD received signal from the kth TE is given as

$$\begin{aligned}\tilde{y}_{k,n,u} = \mathbf{p}_{k,n,u}^H \tilde{\mathbf{h}}_{k,n}^{\{B_{r_0}\}} x_{k,u} + \sum_{i=1, i\neq k}^{K} \mathbf{p}_{k,n,u}^H \tilde{\mathbf{h}}_{i,n}^{\{B_{r_0}\}} x_{i,u} \\ + \mathbf{p}_{k,n,u}^H \tilde{\mathbf{n}}_u^{\{B_{r_0}\}} \end{aligned} \tag{42}$$

where the second item on the right side of (42) is the multiuser interference resulting from imperfect CSI. Based on (42), the SINR of the signal can be written as

$$\gamma_{k,n,u} = \frac{p_{u,k} \left\| \mathbf{p}_{k,n,u}^H \tilde{\mathbf{h}}_{n,k}^{\{B_{r_0}\}} \right\|^2}{\sum_{i=1, i\neq k}^{K} p_{u,i} \left\| \mathbf{p}_{k,n,u}^H \tilde{\mathbf{h}}_{n,i,f_D}^{\{B_{r_0}\}} \right\|^2 + \left\| \mathbf{p}_{k,n,u}^H \tilde{\mathbf{n}}_u^{\{B_{r_0}\}} \right\|^2}. \tag{43}$$

Similarly, in downlink, the hybrid beamforming matrix is given as

$$\mathbf{W}_{n,d} = \mathbf{B}_{n,d} \mathbf{\Phi}_{n,d} \mathbf{P}_{n,d}. \tag{44}$$

Based on (17) and (39), the downlink received signal is given as

$$\begin{aligned}\tilde{\mathbf{y}}_{n,d} &= \mathbf{H}_{n,f_D}^H \mathbf{W}_{n,d} \mathbf{x}_d + \mathbf{n}_d \\ &= \left(\tilde{\mathbf{H}}_n^{\{B_{r_0}\}} \right)^H \mathbf{P}_{n,d} \mathbf{x}_d + \mathbf{n}_d \end{aligned} \tag{45}$$

$$\begin{aligned}\tilde{y}_{k,n,d} = \left(\tilde{\mathbf{h}}_{k,n}^{\{B_{r_0}\}} \right)^H \mathbf{p}_{k,n,d} x_{k,d} \\ + \sum_{i=1, i\neq k}^{K} \left(\tilde{\mathbf{h}}_{k,n}^{\{B_{r_0}\}} \right)^H \mathbf{p}_{i,n,d} x_{i,d} + n_{k,d}. \end{aligned} \tag{46}$$

Then, the SINR at the kth TE is given as

$$\gamma_{k,n,d} = \frac{p_{k,d} \left\| \tilde{\mathbf{h}}_{k,n}^{\{B_{r_0}\}} \mathbf{p}_k \right\|^2}{\sum_{i=1, i\neq k}^{K} p_{i,d} \left\| \tilde{\mathbf{h}}_{k,n}^{\{B_{r_0}\}} \mathbf{p}_i \right\|^2 + \sigma_{d,k}^2}. \tag{47}$$

According to the Shannon equation, the ergodic sum rate is given by

$$R_{n,a} = \mathbb{E} \left\{ \sum_{k=1}^{K} \log_2 \left(1 + \gamma_{k,n,a} \right) \right\}, a \in \{u, d\}. \tag{48}$$

To fairly evaluate the system performance, we consider the sum SE. Let n_t be the number of transmitted symbols in an AOAT, and during each AOAT, n_τ symbols are used for training. Therefore, the sum SE is given by

$$SE = \frac{n_t - n_\tau}{n_t} \left(R_{n,u} + R_{n,d} \right). \tag{49}$$

VI. Analysis of Pilot Overhead and Computational Complexity

In this section, we perform comparisons of the pilot overhead and computational complexity. From the above discussion, the pilot overhead is evaluated by n_τ, which is further determined by the length of each pilot sequence and the time of transmitting the pilot. For normal estimation, such as MMSE or LS, τ is equal to the number of TEs K. The pilot overhead is $n_\tau = N_m K^2$. For the user grouping and pilot reuse schemes in the BD [34], [40], τ is equal to the number of groups G ($G \ll K$). The pilot overhead is $n_\tau = N_m K G$, which is considerably lower than the normal estimation overhead. Similarly, in the AD channel tracking scheme, the pilot overhead is given as $n_\tau = {N'}_m K G$. The only difference lies in the increase in the number of times the pilot is transmitted (${N'}_m \geq N_m$). To a certain degree, the proposed AD tracking scheme is designed to make a tradeoff between training overhead and estimation quality. Compared with the FD training method, the pilot overhead is rather small.

We now discuss the computational complexity from three aspects: AOA estimation, CSI acquisition, and hybrid beamforming. First, the computational complexity of proposed beam alignment method is compared with that of the multiple signal classification (MUSIC) algorithm [47] and the estimation of signal parameters via rotational invariance techniques (ESPRIT) algorithm [48]. The proposed beam alignment method includes two parts, i.e., M-points DFT and local oversampling around the beam index with maximal gain. The whole process can be realized in DSP module and the computational complexity is $\mathcal{O}\left(M\left(M+N\right)\right)$. The main step of MUSIC and ESPRIT algorithms includes three parts, i.e., covariance matrix construction $\mathcal{O}\left(M^2 T_s\right)$, eigenvalue decomposition $\mathcal{O}\left(M^3\right)$, and spectrum search $\mathcal{O}\left(DM^3\right)$. The whole computational complexity is $\mathcal{O}\left(M^2 T_s + M^3 + DM^3\right)$, where T_s is the number of snapshot and D is the search dimension of angle. Comparing the result with that from MUSIC and ESPRIT, we can find that the computational complexity of the proposed method is lower than that of MUSIC and ESPRIT, when $N < M^2$. This condition is guaranteed in practical mMIMO system.

Then, the computational complexities of the proposed channel tracking schemes are compared with those of the LS and MMSE estimation methods. The comparison results are shown in Table II. The computational complexity of channel training and beamforming is determined by accumulated number of addition and multiplication. According to the acquisition of (29), the complexity of LS method is related to channel dimension, $\mathcal{O}\left(M\right)$. Similar to LS method, matched filter (MF) obtains the same performance. The complexity of ZF and MMSE is mainly determined by the inversion of K-order matrix [49], whose complexity reaches $\mathcal{O}\left(K^3\right)$. The multipath channel tracking scheme has the largest computational complexity, resulting from the inverse production of the Kalman factor matrix, whereas the AD tracking scheme has the lowest complexity with the LS method because only the strongest beam gain is tracked. The computation of the AD tracking scheme mainly arises from the DFT transformation from the pilot signals in (33).

Finally, a comparison of the complexity of beamforming is performed between the hybrid and linear methods, both of which include three schemes, i.e., MF, ZF, and MMSE. The result is shown in Table III. As shown in this table, the complexity of the linear method increases with increasing number of antennas, which introduces the challenge of high-dimensional channel management and complicated transceiver design. However, the complexity of the hybrid method is only associated with the number of TEs because the angular beamforming matrix only chooses K aligned beams, which can easily be realized by using

TABLE II
COMPUTATIONAL COMPLEXITIES OF DIFFERENT CSI ACQUISITION METHODS

CSI Acquisition	full-dimensional channel estimation		Kalman channel tracking	
	LS	MMSE	multipath channel tracking	angle-domain channel tracking
Computational Complexity	$\mathcal{O}(M)$	$\mathcal{O}(M+K^3)$	$\mathcal{O}(M^3)$	$\mathcal{O}(M)$

TABLE III
COMPUTATIONAL COMPLEXITIES OF DIFFERENT BEAMFORMING METHODS

Beamforming Scheme		MF	ZF	MMSE
Computational Complexity	linear method	$\mathcal{O}(M)$	$\mathcal{O}(M+K^3)$	$\mathcal{O}(M+K^3)$
	angle domain aided method	$\mathcal{O}(K)$	$\mathcal{O}(K^3)$	$\mathcal{O}(K^3)$

KF low-cost phase shifters in the analog domain. Meanwhile, the dimension of the BD beamforming matrix is suppressed from M to K, which can be implemented in the digital domain. Thus, the hybrid beamforming method makes the computation robust irrespective of how the number of antennas varies at the BS. A similar result can be obtained when comparing with the BD method.

In general, the AD channel tracking scheme not only has a relatively low pilot overhead but also surpasses the FD channel estimation method in terms of computational complexity. Meanwhile, compared with the linear and BD methods, the corresponding AD-aided hybrid beamforming method has lower complexity.

VII. SIMULATION RESULTS

In this section, the performance of the AD channel tracking and hybrid beamforming scheme is evaluated through simulations. We consider a TDD mMIMO system in the HSR scenario, where the BS has $M = 128$ antennas. A total of $K = 16$ TEs are uniformly distributed on the top of the train in uniform intervals of 25 m. The vertical distance from the BS to the rail track is $d_0 = 250$ m. The moving speed of the train is $v = 350$ km/h. According to the measurement of AOA characteristics [21], the AS is set to be 20°. We mainly consider the viaduct scenario, and the Rician factor is $\mathcal{K} = 22.75$ dB [20]. The channel fading coefficients are generated from the 3GPP spatial channel model for MIMO simulation [50]. The number of paths is $L = 20$, and the pass loss is given as $PL_{LoS}\,(dB) = 34.53 + 38\log 10(d)$ and $PL_{NLoS}\,(dB) = 30.18 + 26\log 10(d)$. Additionally, a bulk normal shadowing applied to subpaths has a standard of deviation of 4 dB. The carrier frequency is $f_c = 1.9$ Ghz, and the noise variance is -92 dBm.

Define $\mathbb{E}\{\|\mathbf{h}_{k,n} - \hat{\mathbf{h}}_{k,n}\|^2 / \|\mathbf{h}_{k,n}\|^2\}$ as the mean square error (MSE). The performance of the AD channel tracking scheme is shown in Fig. 5. Under low signal-to-noise ratio (SNR) conditions, the AD channel tracking scheme obtains the best performance. The MSE of the proposed scheme is influenced by oversampling factor N because more accurate phase rotation will lead to less power leakage and more precise channel reconstruction. Increasing the number of iteration will introduce quick convergence to lower bound, while the cost is more consumption of pilot signals and time resources. In the HSR scenarios, using this method should be avoided. Under high SNR conditions, the performance of AD tracking scheme converges to lower bound, which mainly comes from the approximation error with one beam. Increasing the oversampling factor helps to decrease the lower bound and further improve channel tracking accuracy. Without compressing the channel dimension, the FD tracking scheme surpasses the AD scheme and obtains lower MSE under high SNR conditions. Compared with FD tracking scheme, the performance constraint of traditional LS method mainly comes from additional phase error from DFO. The performance of the AOA tracking scheme [26] depends on the accuracy of double approximation of channel: one is made for estimating the AOA, and the other is made for recovering the CSI. The high bound of the KF tracking scheme [12] mainly comes from the blind prediction of the channel.

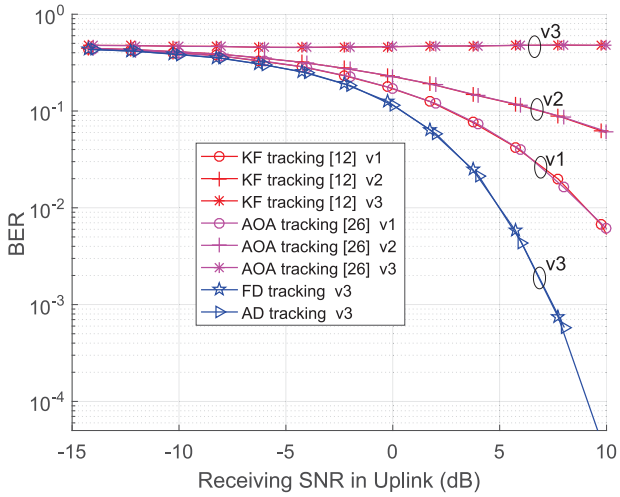

Fig. 6. BER in uplink. $v1 = 50$ km/h, $v2 = 100$ km/h, $v3 = 300$ km/h. Modulation: QPSK (without Gray Mapping).

Fig. 6 shows the relationship between BER and receiving SNR under different speed conditions. When train moves in low speed, the performance is mainly determined by receiving SNR. Increasing the transmission power of signal helps to decrease BER. However, under high-speed moving conditions, this method fails since BER performance is mainly determined by DFO compensation effect. By aligning beams toward users' azimuth angles, accurate AOA is acquired and DFO is well compensated. Thus the proposed AD tracking scheme obtains the best performance. When satisfying a specific BER requirement, the AD tracking scheme can significantly reduce the transmission power and improve the energy efficiency.

Fig. 7 shows the ergodic sum rate of the hybrid beamforming scheme, in which both CSI acquisition and transmission are considered. During the 1st and 2nd CTs, the proposed AD tacking scheme obtains the highest throughput. The performance of the FD tracking scheme is close to that of the AD tracking scheme, while the corresponding pilot overhead and complexity are much larger. Based on the compression level of channel

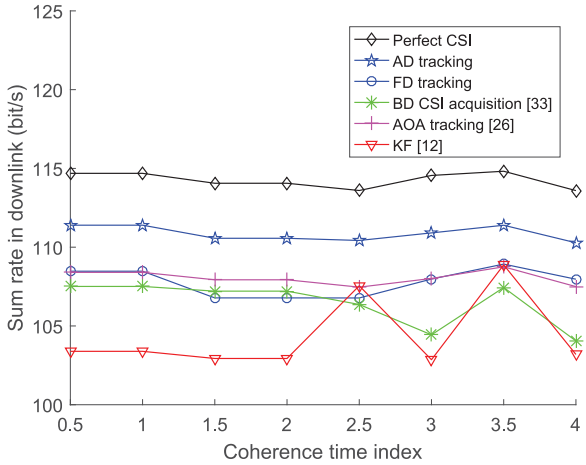

Fig. 7. Ergodic sum rate in downlink. The mean receiving SNR is 30 dB. CSI mutates in the third and fourth CTs.

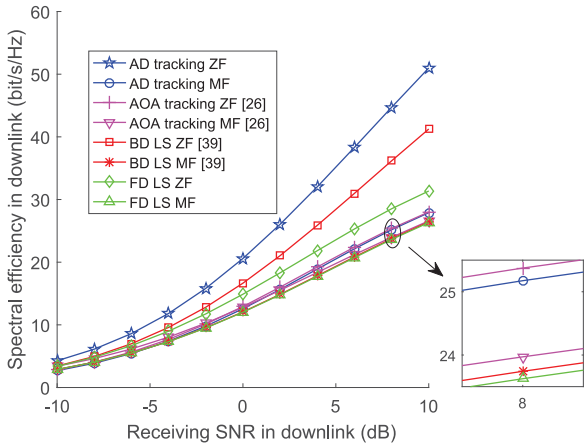

Fig. 8. SE versus receiving SNR. $M = 128$, and $n_t = 1024$.

dimension, the BD solution [34] can be viewed as a tradeoff between training overhead and throughput. According to the discussions about Fig. 5, the performance of different schemes lies in the CSI estimation error. When CSI mutates in the next two CTs, both the normal BD CSI acquisition [34] and KF tracking scheme [12] suffer from fluctuations in data rate, while the proposed AD tracking scheme is self-adaptive to vulnerable CSI and maintains a high throughput at the cost of increasing limited pilot overhead.

Fig. 8 compares the SE of BD transmission scheme [40] and AD-aided hybrid beamforming scheme. Both the training and transmission are considered. It shows that the performance of ZF is better than that of MF because when receiving SNR is large, the performance of the system is limited by interuser interference. Under ZF conditions, the interference from other TEs can be projected to zero space and the SINR of desired signal is improved. The AD tracking scheme obtains the best SE since the least pilot overhead is consumed. The FD linear ZF method obtains the lowest performance. In practice, Using this method will cause high hardware overhead and computational complexity, which is difficult for engineering implement. Compared with the AD tracking scheme and the FD LS scheme, BD transmission method [40] makes a tradeoff about the pilot overhead, which is suitable for general communication scenario. Under strong Rician-channel condition, AD method can obtain the optimal performance by utilizing temporal correlation.

VIII. Conclusion

In this paper, we proposed an AD channel tracking and hybrid beamforming scheme for HSR communications. The spatial property was investigated to decompose the channel into spatial angular information and beam gain. First, the angular information was captured by performing FFT oversampling to align the beam toward the exact direction of signals, based on which the DFO was compensated. Then, a linear KF was applied to track time-varying beam gain and recover the FD channel. The training overhead was significantly reduced, while the tracking scheme was still robust and self-adaptive to vulnerable CSI conditions. The hybrid beamforming included three parts: DFO compensation, angular beamforming, and BD reception/precoding. The angular beamforming was realized in the AD with limited phase shifters, while the BD reception/precoding was implemented in the digital domain, whose complexity was the lowest. The numerical results showed that the proposed AD tracking scheme and hybrid beamforming obtained the best performance.

References

[1] J. Wu and P. Fan, "A survey on high mobility wireless communications: Challenges, opportunities, and solutions," *IEEE Access*, vol. 4, pp. 450–476, 2016.

[2] R. He *et al.*, "High-speed railway communications: from GSM-R to LTE-R" *IEEE Veh. Technol. Mag.*, vol. 11, no. 3, pp. 49–58, Sep. 2016.

[3] Y. Lu, K. Xiong, P. Fan, and Z. Zhong, "Optimal multicell coordinated beamforming for downlink high-speed railway communications," *IEEE Trans. Veh. Technol.*, vol. 66, no. 10, pp. 9603–9608, Oct. 2017.

[4] F. Rusek *et al.*, "Scaling up MIMO: Opportunities and challenges with very large arrays," *IEEE Signal Process. Mag.*, vol. 30, no. 1, pp. 40–60, Jan. 2013.

[5] J. Hoydis, S. Brink, and M. Debbah, "Massive MIMO in UL/DL of cellular networks: How many antennas do we need?" *IEEE J. Sel. Areas Commun.*, vol. 31, no. 2, pp. 160–171, Feb. 2013.

[6] H. Q. Ngo, E. G. Larsson, and T. L. Marzetta, "Energy and spectral efficiency of very large multiuser MIMO systems," *IEEE Trans. Commun.*, vol. 61, no. 4, pp. 1436–1449, Apr. 2013.

[7] T. L. Marzetta, "Noncooperative cellular wireless with unlimited numbers of BS antennas," *IEEE Trans. Wireless Commun.*, vol. 9, no. 11, pp. 3590–3600, Nov. 2010.

[8] X. Chen, J. Lu, T. Li, P. Fan, and K. B. Letaief, "Directivity-beamwidth tradeoff of massive MIMO uplink beamforming for high speed train communication," *IEEE Access*, vol. 5, pp. 5936–5946, 2017.

[9] X. Chen, J. Lu, S. Liu, and P. Fan, "Location-aided umbrella-shaped massive MIMO beamforming scheme with transmit diversity for high speed railway communications," in *Proc. IEEE 83rd Veh. Technol. Conf.*, Nanjing, China, 2016, pp. 1–5.

[10] T. Li, X. Wang, P. Fan, and T. Riihonen, "Position-aided large-scale MIMO channel estimation for high-speed railway communication systems," *IEEE Trans. Veh. Technol.*, vol. 66, no. 10, pp. 8964–8978, Oct. 2017.

[11] X. Liu and D. Qiao, "Location-fair beamforming for high speed railway communication systems," *IEEE Access*, vol. 6, pp. 28632–28642, 2018.

[12] C. Zhang, J. Zhang, Y. Huang, and L. Yang, "Location-aided channel tracking and downlink transmission for HST massive MIMO systems," *IET Commun.*, vol. 11, no. 13, pp. 2082–2088, 2017.

[13] J. Wang, H. Zhu, and N. J. Gomes, "Distributed antenna systems for mobile communications in high speed trains," *IEEE J. Sel. Areas Commun.*, vol. 30, no. 4, pp. 675–683, May 2012.

[14] L. Zhou, Z. Yang, F. Luan, A. F. Molisch, F. Tufvesson, and S. Zhou, "Dynamic channel model with overhead line poles for high-speed railway communications," *IEEE Antennas Wireless Propagation Lett.*, vol. 17, no. 5, pp. 903–906, May 2018.

[15] R. Zeng, H. Huang, L. Yang, and Z. Zhang, "Joint estimation of frequency offset and doppler shift in high mobility environments based on orthogonal angle domain subspace projection," *IEEE Trans. Veh. Technol.*, vol. 67, no. 3, pp. 2254–2266, Mar. 2018.

[16] Y. GE, W. Zhang, and F. Gao, "High-mobility OFDM downlink transmission with partly calibrated subarray-based massive uniform linear array," in *Proc. IEEE 85th Veh. Technol. Conf.*, Sydney, Australia, 2017, pp. 1–6.

[17] W. Guo, W. Zhang, P. Mu, F. Gao, and B. Yao, "Angle-domain Doppler pre-compensation for high-mobility OFDM uplink with massive ULA," in *Proc. IEEE Global Commun. Conf.*, 2017, pp. 1–6.

[18] T. Liu, X. Ma, R. Zhao, H. Dong, and L. Jia, "Doppler shift estimation for high-speed railway scenario," in *Proc. IEEE 83rd Veh. Technol. Conf.*, Nanjing, China, 2016, pp. 1–5.

[19] D. He *et al.*, "Channel measurement, simulation, and analysis for high-speed railway communications in 5G millimeter-wave band," *IEEE Trans. Intell. Transp. Syst.*, vol. 19, no. 10, pp. 2254–2266, Oct. 2018.

[20] Y. Zhao, X. Wang, G. Wang, R. He, Y. Zou, and Z. Zhao, "Channel estimation and throughput evaluation for 5G wireless communication systems in various scenarios on high speed railways," *China Commun.*, vol. 15, no. 4, pp. 86–97, Apr. 2018.

[21] T. Zhou, C. Tao, S. Salous, and L. Liu, "Measurements and analysis of angular characteristics and spatial correlation for high-speed railway channels," *IEEE Trans. Intell. Transp. Syst.*, vol. 19, no. 2, pp. 357–367, Feb. 2018.

[22] T. Zhou, C. Tao, S. Salous, and L. Liu, "Spatial characterization for high-speed railway channels based on moving virtual array measurement scheme," *IEEE Antennas Wireless Propag. Lett.*, vol. 16, pp. 1423–1426, 2017.

[23] X. Ma, F. Yang, and J. Song, "Time-angle domain sparsity based MIMO channel estimation approach in high mobility scenarios," *IEEE Commun. Lett.*, vol. 22, no. 9, pp. 1946–1949, Sep. 2018.

[24] C. Komninakis *et al.*, "Multi-input multi-output fading channel tracking and equalization using Kalman estimation," *IEEE Trans. Signal Process.*, vol. 50, no. 5, pp. 1065–1075, Dec. 2010.

[25] W. Santipach and M. L. Honig, "Optimization of training and feedback overhead for beamforming over block fading channels," *IEEE Trans. Inf. Theory*, vol. 56, no. 12, pp. 6103–6115, Dec. 2010.

[26] J. Zhao, F. Gao, W. Jia, S. Zhang, S. Jin, and H. Lin, "Angle domain hybrid precoding and channel tracking for millimeter wave massive MIMO systems," *IEEE Trans. Wireless Commun.*, vol. 16, no. 10, pp. 6868–6880, Oct. 2017.

[27] J. Zhao, H. Xie, F. Gao, W. Jia, S. Jin, and H. Lin, "Time varying channel tracking with spatial and temporal BEM for massive MIMO systems," *IEEE Trans. Wireless Commun.*, vol. 17, no. 8, pp. 5653–5666, Oct. 2017.

[28] J. Talvitie, T. Levanen, M. Koivisto, K. Pajukoski, M. Renfors, and M. Valkama, "Positioning of high-speed trains using 5G new radio synchronization signals," in *Proc. IEEE Wireless Commun. Netw. Conf.*, Barcelona, Spain, 2018, pp. 1–6.

[29] P. Kela *et al.*, "Location based beamforming in 5G ultra-dense networks," in *Proc. IEEE 84th Veh. Technol. Conf.*, Montreal, QC, Canada, 2016, pp. 1–7.

[30] T. Zhou, C. Tao, L. Liu, and Z. Tan, "Ricean K-factor measurements and analysis for wideband high-speed railway channels at 2.35 GHz," *Radioengineering*, vol. 23, no. 2, pp. 578–585, Jun. 2014.

[31] H. Q. Ngo, H. A. Suraweera, M. Matthaiou, and E. G. Larsson, "Multipair full-duplex relaying with massive arrays and linear processing," *IEEE J. Sel. Areas Commun.*, vol. 32, no. 9, pp. 1721–1737, Sep. 2014.

[32] A. Adhikary, J. Nam, J. Y. Ahn, and G. Caire, "Joint spatial division and multiplexing the large-scale array regime," *IEEE Trans. Inf. Theory*, vol. 59, no. 10, pp. 6441–6463, Oct. 2013.

[33] C. Sun, X. Gao, S. Jin, M. Matthaiou, Z. Ding, and C. Xiao, "Beam division multiple access transmission for massive MIMO communications," *IEEE Trans. Commun.*, vol. 63, no. 6, pp. 2170–2184, Jun. 2015.

[34] X. Xia, K. Xu, D. Zhang, Y. Xu, and Y. Wang, "Beam-Domain full-duplex massive MIMO: Realizing co-time co-frequency uplink and downlink transmission in the cellular system," *IEEE Trans. Veh. Technol.*, vol. 66, no. 10, pp. 8845–8862, Oct. 2017.

[35] H. Lin, F. Gao, S. Jin, and G. Y. Li, "A New view of multi-user hybrid massive MIMO: Non-orthogonal angle division multiple access," *IEEE J. Sel. Areas Commun.*, vol. 35, no. 10, pp. 2268–2280, Oct. 2017.

[36] H. Yin, D. Gesbert, M. Filippou, and Y. Liu, "A coordinated approach to channel estimation in large-scale multiple-antenna systems," *IEEE J. Sel. Areas Commun.*, vol. 31, no. 2, pp. 264–273, Feb. 2013.

[37] J.-A. Tsai, R. M. Buehrer, and B. D. Woerner, "The impact of AOA energy distribution on the spatial fading correlation of linear antenna array," in *Proc. IEEE 55th Veh. Technol. Conf.*, 2002, vol. 2, pp. 933–937.

[38] W. Guo, W. Zhang, P. Mu, F. Gao, and B. Yao, "Angle-domain doppler pre-compensation for high-mobility OFDM uplink with massive ULA," in *Proc. IEEE Global Commun. Conf.*, Singapore, 2017, pp. 1–6.

[39] W. Guo, W. Zhang, P. Mu, and F. Gao, "High-mobility OFDM downlink transmission with large-scale antenna array," *IEEE Trans. Veh. Technol.*, vol. 66, no. 9, pp. 8600–8604, Sep. 2017.

[40] H. Xie, F. Gao, S. Zhang, and S. Jin, "A unified transmission strategy for TDD/FDD massive MIMO systems with spatial basis expansion model," *IEEE Trans. Veh. Technol.*, vol. 66, no. 4, pp. 3170–3184, Apr. 2017.

[41] W. Luo, X. Fang, M. Cheng, and Y. Zhao, "Efficient multiple-group multiple-antenna (MGMA) scheme for high-speed railway viaducts," *IEEE Trans. Veh. Technol.*, vol. 62, no. 6, pp. 2558–2569, Jul. 2013.

[42] A. Abdi and M. Kaveh, "A space-time correlation model for multielement antenna systems in mobile fading channels," *IEEE J. Sel. Areas Commun.*, vol. 20, no. 3, pp. 550–560, Apr. 2002.

[43] A. Abdi, J. A. Barger, and M. Kaveh, "A parametric model for the distribution of the angle of arrival and the associated correlation function and power spectrum at the mobile station," *IEEE Trans. Veh. Technol.*, vol. 51, no. 3, pp. 425–434, May 2002.

[44] V. Va, J. Choi, and R. W. Heath, "The impact of beamwidth on temporal channel variation in vehicular channels and its implications," *IEEE Trans. Veh. Technol.*, vol. 66, no. 6, pp. 5014–5029, Jun. 2017.

[45] C. Komninakis, C. Fragouli, A. H. Sayed, and R. D. Wesel, "Multi-input multi-output fading channel tracking and equalization using Kalman estimation," *IEEE Trans. Signal Process.*, vol. 50, no. 5, pp. 1065–1076, May 2002.

[46] T. Kailath, A. H. Sayed, and B. Hassibi, *Linear Estimation*. Englewood Cliffs, NJ, USA: Prentice-Hall, 2000.

[47] R. Schmidt, "Multiple emitter location and signal parameter estimation," *IEEE Trans. Antennas Propag.*, vol. 34, no. 3, pp. 276–280, Mar. 1986.

[48] A. J. Weiss and M. Gavish, "Direction finding using ESPRIT with interpolated arrays," *IEEE Trans. Signal Process.*, vol. 39, no. 6, pp. 1473–1478, Jun. 1991.

[49] S. M. Kay, *Fundamentals of Statistical Signal Processing: Estimation Theory*. Englewood Cliffs, NJ, USA: Prentice-Hall, 1993.

[50] J M Meredith, "Spatial channel model for multiple input multiple output (MIMO) simulations," Tech-invite, Tech Rep. TR 25.996, Version 13.0.0, Jan. 13, 2016.